JACS
JOURNAL OF THE AMERICAN CHEMICAL SOCIETY
Communication
pubs.acs.org/JACS

Supported Tetrahedral Oxo-Sn Catalyst: Single Site, Two Modes of Catalysis

Evgeny V. Beletskiy,[†] Xianliang Hou,[†,⊥] Zhongliang Shen,[†] James R. Gallagher,[§] Jeffrey T. Miller,[∥] Yuyang Wu,[‡] Tiehu Li,[⊥] Mayfair C. Kung,*[,†] and Harold H. Kung*[,†]

[†]Chemical and Biological Engineering and [‡]Chemistry Department, Northwestern University, Evanston, Illinois 60208, United States
[§]Chemical Sciences Division, Argonne National Laboratory, Naperville, Illinois 60429, United States
[∥]Chemical Engineering Department, Purdue University, West Lafayette, Indiana 47907, United States
[⊥]Northwestern Polytechnical University, Xi'an, Shaanxi 710072, PR China

Supporting Information

ABSTRACT: Mild calcination in ozone of a (POSS)-Sn-(POSS) complex grafted on silica generated a heterogenized catalyst that mostly retained the tetrahedral coordination of its homogeneous precursor, as evidenced by spectroscopic characterizations using EXAFS, NMR, UV−vis, and DRIFT. The Sn centers are accessible and uniform and can be quantified by stoichiometric pyridine poisoning. This Sn-catalyst is active in hydride transfer reactions as a typical solid Lewis acid. However, the Sn centers can also create Brønsted acidity with alcohol by binding the alcohol strongly as alkoxide and transferring the hydroxyl H to the neighboring Sn−O−Si bond. The resulting acidic silanol is active in epoxide ring opening and acetalization reactions.

Many important industrial Lewis acid catalyzed reactions use homogeneous Lewis acids, although solid Lewis acids offer advantages in the ease of handling, separation, and regeneration.[1−4] Among solid Lewis acids, Sn-Beta zeolite is heavily investigated because of its thermal stability, water tolerance, and ability to catalyze many selective transformations, even in aqueous media.[5−10] The active sites in Sn-Beta are isolated, tetrahedrally coordinated (T_d) Sn[11] and possess properties distinct from the octahedral (O_h) Sn in small SnO_2 clusters that were generated in the channels and on the outer surface of the beta zeolite.[12,8,13] Size constraint due to the small channels of zeolite has led to efforts to incorporate Sn into mesoporous silica, but often there is a distribution of Sn species in these materials, especially at higher metal loadings.[14,15]

Here we report the synthesis of a solid Lewis acid with uniform T_d Sn(IV) centers supported on a high-surface-area nonporous silica. These Sn centers were Lewis acids that catalyzed many reactions including a Meerwein−Ponndorf−Verley reaction, epoxide ring opening, acetal formation, and glucose isomerization. Because the support was nonporous, the catalyst was also active in converting cellobiose to hydroxymethylfurfural (HMF). This is a reaction in which the reactant molecule is too large to be processed efficiently inside a beta zeolite channel,[16] and breaking it down into individual monosaccharides with the aid of HCl[17] or high temperature[18] is typically required prior to a Sn-catalyzed transformation. Mechanistic investigations utilizing poisoning experiments, DRUV−vis, DRIFTS, and solid-state NMR revealed that the reactions proceed via either Lewis acid catalysis or a less typical Lewis acid-assisted Brønsted acid catalysis, thus demonstrating an unusual case of dual-mode catalytic reactivity of a single-site catalyst.

The catalysts were prepared (Scheme 1) by hydrosilylating a T_d Sn complex **I**, $[(c\text{-}C_6H_{11})_7Si_7O_9(OSi(CH_3)_2(C_2H_3))O_2]_2Sn$ (abbreviated as (POSS)-Sn-(POSS)), synthesized according to our previous work,[19] onto dimethylsilane-modified EH-5 fumed silica. The hydrosilylation reaction conditions under which **I** retained its structural integrity were determined using NMR with a model reaction of **I** with 1,1,3,3,5,5-hexamethyltrisiloxane that served as a surrogate for silica (Figure S1). CPMAS ^{119}Sn NMR spectrum of **II** exhibited a single resonance at −439 ppm (Figure S2a) characteristic of T_d Sn, although the signal-to-noise ratio was low. Successful retention of the POSS-Sn-POSS structure was also supported by EXAFS analysis (Table

Scheme 1. Preparation of Silica-Supported Catalysts II and III

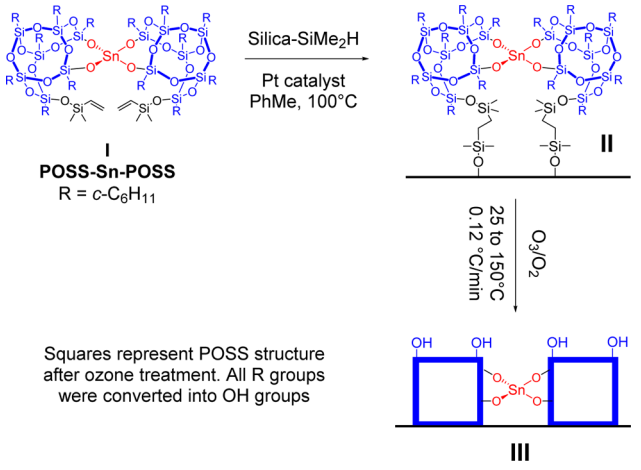

Received: December 23, 2015
Published: March 17, 2016

DOI: 10.1021/jacs.5b13436
J. Am. Chem. Soc. 2016, 138, 4294−4297

S1 and Figure S2b), which showed a Sn coordination of 3.5 ± 0.4 in **II**. The DRIFT spectrum showed sharp peaks in the C−H stretch region of 2800−3000 cm^{-1} from the cyclohexyl groups of POSS and the methylsilyl groups on SiO_2 (Figure S3a).

III was formed by calcination of **II** in a flow of O_2 and O_3 mixture under mild temperature conditions to avoid possible decomposition or rearrangement of the Sn centers. After calcination, all organic functionalities attached to Si were oxidized to SiOH as indicated by DRIFT (Figure S3a). EXAFS of **III** showed that the Sn−O scattering increased slightly relative to that of **II**, and the average coordination number became 4.5 ± 0.4 (Figure S3b and Table S1). There was a trace amount of higher shells scattering, which may be due to SnO_x clusters resulting from "opening" of the tin sites with the water vapors forming during the calcination process. This indicated that there might have existed ca. 25% octahedral Sn as isolated center or SnO_2-type material, although the majority of the species were predominantly single-site, T_d Sn. The EXAFS result was consistent with the UV−vis spectrum, which showed an absorption peak at ∼210 nm (Figure S8d), characteristic of charge transfer from O^{2-} to T_d Sn^{4+}.[20] It should be noted that the absorption in the 283 nm region typical for O_h Sn was not detectable for either **II** or **III**.[21,22] The Sn loading of **III** was 1.1 wt % as determined by ICP, translating into 90 μmol **I**/g SiO_2 grafted, in line with the amount of **I** that disappeared from the solution after hydrosilylation. On the basis of the footprint of **I** of 2.5 nm^2 (from the single-crystal X-ray data)[19] and a surface area of silica of 190 m^2/g, the surface coverage of **II** was estimated to be 70%.

The accessibility of Sn in **II** and **III** to pyridine (py) was investigated with DRIFT (Figures S4 and S5). After the sample was exposed to py vapor and He purged at 150 °C at a low flow rate, peaks ascribed to physisorbed/hydrogen-bonded py (1445 and 1597 cm^{-1}) and py coordinated to Lewis acid sites (1456, 1491, 1577, and 1613 cm^{-1})[23] were detected for both samples. Trace amounts of py adsorbed on Brønsted acid sites (1550 and 1640 cm^{-1}) were also detected for **III**. The physisorbed and hydrogen-bonded species were associated with the silica support and could be removed with a high purging rate at 150 °C (Figure S5a). The remaining py bonded to Sn could be displaced by aqueous NaOH, extracted into $CDCl_3$, and quantified with ^1H NMR. The ratio of py to Sn was ca. 1:1 at 150 °C but decreased at higher temperature or prolonged heating because of desorption from the Sn Lewis acid site (Table S2).

The catalytic properites were examined using styrene oxide ring opening with a 15-fold excess of 2-propanol. For **III**, the reaction proceeded readily at 50 °C with an apparent first-order kinetics in epoxide concentration. The apparent rate constant was 2.0×10^{-2} min^{-1}, which was equivalent to 2.2×10^5 min^{-1} $(mol\ Sn)^{-1}$ and TON = 490 at 40 min (Tables S5 and S6), whereas **II** showed only moderate reactivity at 80 °C with k_e= 8.6×10^2 min^{-1} $(mol\ Sn)^{-1}$. The effect of Sn loading was investigated with a lower Sn loading sample (**III-low** with 0.21 wt % Sn). Its activity per Sn (k_e= 1.6×10^5 min^{-1} $(mol\ Sn)^{-1}$) was only 25% lower than that of **III**, implying within uncertainties presence of mostly isolated Sn centers in **III**. This was consistent with the structure of Sn center sandwiched between bulky POSS ligands. Contribution of leached Sn to the reaction of **III** was excluded by conducting the reaction at room temperature to different conversions in two separate experiments and removing the catalyst by filtration, then observing that the reaction stopped completely (Figure S9). If benzyl alcohol was used as the nucleophile instead of 2-propanol, then the difference between **II** and **III** was even larger. The conversion was complete within 10 min at room temperature using **III** (TON = 950) but was only 50% after 3 h at 80 °C with **II**.

Py poisoning of the reaction of styrene oxide with 2-propanol was used to quantify and probe the uniformity of Sn. The reaction remained pseudo-first-order in styrene oxide up to high conversions even in the presence of py (Tables S5 and S6 and Figure S8a). The exception was at the highest py/Sn ratio of 54%, when the data deviated from pseudo-first-order kinetics after 30 min for reasons yet to be investigated (Figure S8a), and only initial data were used in calculating k_e. The rate constants decreased linearly with increasing py, as shown in Figure 1,

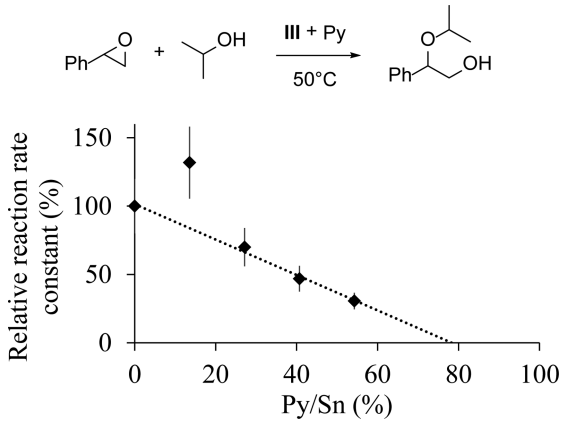

Figure 1. Effect of the pyridine poisoning on the apparent rate constant of the styrene oxide ring opening with 2-propanol (from Table S5).

suggesting homogeneity of the Sn centers. Extrapolation of the data showed that complete poisoning would occur at py/Sn ≈ 80%, indicating that most of the Sn were active, which was consistent with the 4.5 average coordination from the EXAFS data and the fact that a large majority of Sn was present as T_d Sn. The higher than expected k_e at ∼15% py/Sn was repeatable, and further work is needed to understand this.

The quantitaive poisoning of Sn by py was surprising in view of the 10^5 excess of alcohol to py and the results of the following competitive binding experiment. The ^{13}C CPMAS NMR of 2-propanol adsorbed on **III** showed two broadened resonances at 67 and 22.5 ppm (Figure S8b), which were similar to those of Sn 2-propoxide (Figure S8c) but shifted from those of 2-propanol on silica. They did not appear to change upon addition of py, implying that the alkoxide was not displaced by py. Interestingly, py bound to the alkoxide-covered surface at a ∼1.1 Sn:py ratio (Supporting Information, section Vc). DRIFT spectra revealed that this py was bound to H^+ as a pyridium ion with characteristic peaks at 1491, 1546, 1617, and 1638 cm^{-1} (Figure 2, top). UV−vis data showed that the original peak of **III** shifted from ∼210 to ∼233 nm when 2-propanol was adsorbed and dried at 150 °C, consistent with formation of a pentacoordinated geometry of a Sn-2-propanol complex (Figure 2, bottom).[24] A small amount of SnO_2 clusters at 280 nm was also observed, presumably due to hydrolysis of Sn center at higher temperatures. Taken together, these results indicated that 2-propanol adsorbed on **III** as 2-propoxide,

DOI: 10.1021/jacs.5b13436
J. Am. Chem. Soc. 2016, 138, 4294−4297

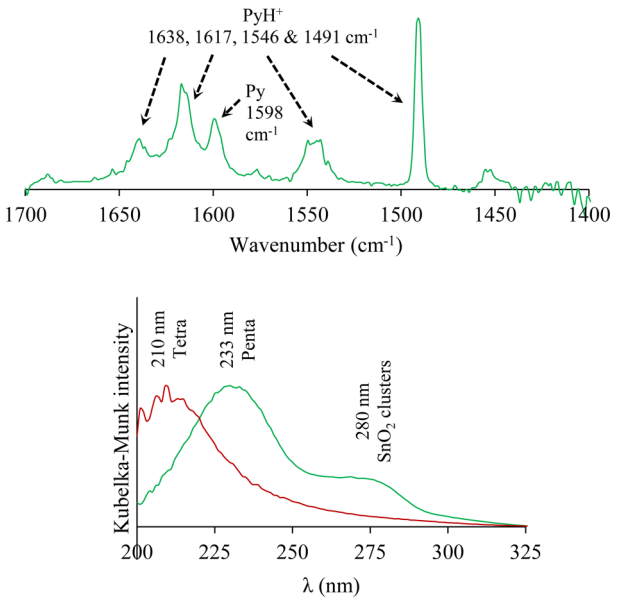

Figure 2. Elucidation of the mechanism of styrene oxide ring opening with 2-propanol. (Top) DRIFT of pyridine adsorbed on **III**-2-propanol. (Bottom) DRUV–vis of **III** (red) and **III**-2-propanol (green).

generating a proton and expanding the coordination sphere without cleaving any of the Sn–O–Si bonds.

We propose the mechanism for the epoxide ring opening with 2-propanol and the effect of py on this reaction as follows (Scheme 2). 2-Propanol was adsorbed onto a Sn center in **III**

Scheme 2. 2-Propanol and Pyridine Binding to III and a Proposed Mechanism of the Epoxide Ring-Opening Reaction and Its Poisoning by Pyridine

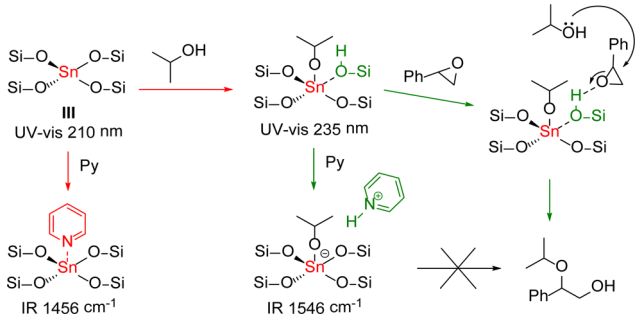

dissociatively as 2-propoxide, whereas the hydroxyl hydrogen was bound to an oxygen of a Sn–O–Si bond. This Sn Lewis acid-activated acidic silanol was the active center in the epoxide ring opening reaction and its binding to py via deprotonation poisoned the reaction. It should be mentioned that under the same conditions neither **I** nor **II** formed any stable alkoxide adducts detectable by NMR presumably due to their steric and hydrophobic properties, and this accounted for their low activity in the epoxide ring-opening reaction.

To verify this proposal, the Meerwein–Ponndorf–Verley hydride-transfer reaction between *p*-nitrobenzaldehyde and benzyl alcohol was examined (Scheme 3, upper path). As established, alcohol binding to Sn in a form of alkoxide was strong for **III**, and it was not displaced by py or weaker bases such as aldehyde. Thus, for **III**, the reaction would proceed via the Sn bound alkoxide.[25,26] The inhibitive effect of py was

Scheme 3. Reaction of *p*-Nitrobenzaldehyde with Benzyl Alcohol via Meerwein–Ponndorf–Verley Hydride Transfer (Upper Path) and Acetal Formation (Lower Path)

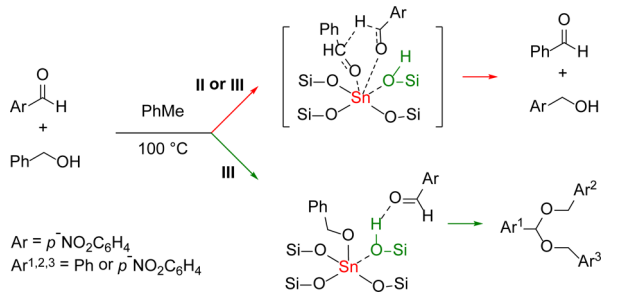

small, as confirmed by the experiments (Table S9), which was also consistent with similar observations reported for solid Zr Lewis acids.[27] **II** also catalyzed hydride transfer (TON ≈ 150 after 16 h for both **II** and **III** in toluene), even though the alcohol binding was weak. Interestingly, the reaction was accelerated in the presence of py (Table S9), and this was presumably due to py shifting the alkoxide binding equilibrium via its deprotonation. Aldehyde and alcohol can also undergo acetal formation (Scheme 3, lower path), but Brønsted acids typically catalyze this reaction. Thus, it was catalyzed by **III** and poisoned by py (Table S8) but not by **II**, similar to the epoxide ring opening reaction.

Interestingly, formation of metal alkoxides via addition of alcohols to M–OSi(H) fragments has previously been observed or proposed;[28–30] however, we could not find a report where it was linked to Brønsted acidity. Instead, the alcohol proton was proposed to react with M–OH to form H_2O.[29,30] Thus, it is quite possible that formation of Brønsted acidity observed in this study also applies to other metal zeolites. For example, Román-Leshkov et al. have reported[30] two different deactivation profiles for a Sn-Beta zeolite catalyst in hydride transfer and etherification reactions, which were thought to proceed via Lewis and Brønsted acid catalyzed pathways, respectively. If the Brønsted acid catalytic activity were originating in Sn-Beta by SiOH binding to Sn in a same way as in **III**, then this could explain the observed drastic deactivation of the catalyst in the etherification process after the "opening" of the Sn centers, which was detected by ^{119}Sn DNP NMR experiments.

Unlike Sn-Beta zeolites, where the Sn sites are located inside the hydrophobic pores, the active centers of **III** are exposed on the surface of the hydrophilic support. Despite this, **III** was active in styrene oxide ring opening by water (TON = 900 after 2 h, 50 °C, Supporting Information, section VII) and in the presence of water generated during acetal production. The TOF in the former reaction was ≥450 h^{-1} for **III** at 50 °C, which was comparable to the literature TOF of 36–400 h^{-1} for ring-opening hydration of various epoxides catalyzed by Sn-Beta catalysts at 40 °C.[31] Thus, the activity of **III** was comparable to Sn-Beta in this epoxide hydration reaction. **III** also catalyzed glucose isomerization in γ-valerolactone at 200 °C (Supporting Information, section VIII), although it was less active than Sn-Beta that was effective at 80 °C for this Lewis acid catalyzed hydride-transfer reaction.[7] The more open configuration of the Sn center in **III** also catalyzed the reaction of large substrates such as cellobiose. In a γ-valerolactone–DMSO mixture at 180 °C, 5-(hydroxymethyl)-furfural was formed with up to 30% yield and TON = 125 (Scheme 4), after cleaving the glucoside bond and isomerizing and dehydrating

DOI: 10.1021/jacs.5b13436
J. Am. Chem. Soc. 2016, 138, 4294–4297

Scheme 4. Cellobiose Conversion into (5-Hydroxymethyl)furfural Catalyzed by III

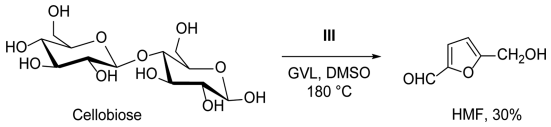

the glucose. In contrast, the reported TON for Sn-Beta in the isomerization of the disaccharide lactose was less than 3.[16]

We have successfully synthesized a uniform, T_d Sn-based Lewis acid catalyst on a nonporous support utilizing a Sn precursor stabilized by a bulky silsesquioxane ligand. The supported Sn catalyst was not only capable of catalyzing typical reactions such as hydride transfer but could also mediate Brønsted acid catalyzed reactions such as epoxide ring opening, acetal formation, and glucoside bond cleavage. The Brønsted acid pathway was suppressed in the presence of bulky hydrophobic substituents and pyridine additive, whereas Lewis acid pathway remained intact, at least in simple hydride-transfer reactions. Thus, two tunable modes of activation are possible for a single catalytic site, and this offers a new avenue in Sn-mediated catalysis.

■ ASSOCIATED CONTENT

Supporting Information

The Supporting Information is available free of charge on the ACS Publications website at DOI: 10.1021/jacs.5b13436.

Experimental procedures, synthesis of materials, EXAFS, NMR, DRIFT and UV−vis spectra, catalyst testing and poisoning experiment details are included in the Supporting Information. (PDF)

■ AUTHOR INFORMATION

Corresponding Authors

*m-kung@northwestern.edu
*hkung@northwestern.edu

Notes

The authors declare no competing financial interest.

■ ACKNOWLEDGMENTS

DOE Office of Basic Energy Sciences, DE-FG02-01ER15184 for support of this work; NUANCE and CleanCat facilities at Northwestern University; MR-CAT at the APS at the Argonne National Laboratory (DE-AC02-06CH11357) for characterization; Cabot Corporation for EH-5 silica sample, X.H. acknowledges support by Chinese Scholarship Fund and partial funding by Institute for Atom-efficient Chemical Transformations (IACT), an Energy Frontier Research Center funded by US DOE Office of Basic Energy Sciences. J.T.M. and J.R.G. were supported by DOE, Office of Basic Energy Sciences, DE-AC-02-06CH11357.

■ REFERENCES

(1) Nakajima, K.; Baba, Y.; Noma, R.; Kitano, M.; Kondo, J. N.; Hayashi, S.; Hara, M. *J. Am. Chem. Soc.* **2011**, *133*, 4224.
(2) Wang, Y.; Wang, F.; Song, Q.; Xin, Q.; Xu, S.; Xu, J. *J. Am. Chem. Soc.* **2013**, *135*, 1506.
(3) Hara, M. *Bull. Chem. Soc. Jpn.* **2014**, *87*, 931.
(4) Ali, M. A.; Siddiki, S. M. A. H.; Kon, K.; Hasegawa, J.; Shimizu, K.-i. *Chem. - Eur. J.* **2014**, *20*, 14256.
(5) Corma, A.; Nemeth, L. T.; Renz, M.; Valencia, S. *Nature* **2001**, *412*, 423.
(6) Corma, A.; Domine, M. E.; Nemeth, L.; Valencia, S. *J. Am. Chem. Soc.* **2002**, *124*, 3194.
(7) Bermejo-Deval, R.; Orazov, M.; Gounder, R.; Hwang, S.-J.; Davis, M. E. *ACS Catal.* **2014**, *4*, 2288.
(8) Pacheco, J. J.; Davis, M. E. *Proc. Natl. Acad. Sci. U. S. A.* **2014**, *111*, 8363.
(9) Renz, M.; Blasco, T.; Corma, A.; Fornés, V.; Jensen, R.; Nemeth, L. *Chem. - Eur. J.* **2002**, *8*, 4708.
(10) Corma, A.; Domine, M. E.; Valencia, S. *J. Catal.* **2003**, *215*, 294.
(11) Bare, S. R.; Kelly, S. D.; Sinkler, W.; Low, J. J.; Modica, F. S.; Valencia, S.; Corma, A.; Nemeth, L. T. *J. Am. Chem. Soc.* **2005**, *127*, 12924.
(12) Bermejo-Deval, R.; Gounder, R.; Davis, M. E. *ACS Catal.* **2012**, *2*, 2705.
(13) Moliner, M.; Roman-Leshkov, Y.; Davis, M. E. *Proc. Natl. Acad. Sci. U. S. A.* **2010**, *107*, 6164.
(14) Alarcon, E. A.; Villa, A. L.; Montes de Correa, C. *Microporous Mesoporous Mater.* **2009**, *122*, 208.
(15) Gaydhankar, T. R.; Joshi, P. N.; Kalita, P.; Kumar, R. *J. Mol. Catal. A: Chem.* **2007**, *265*, 306.
(16) Gounder, R.; Davis, M. E. *J. Catal.* **2013**, *308*, 176.
(17) Nikolla, E.; Román-Leshkov, Y.; Moliner, M.; Davis, M. E. *ACS Catal.* **2011**, *1*, 408.
(18) Holm, M. S.; Pagan-Torres, Y. J.; Saravanamurugan, S.; Riisager, A.; Dumesic, J. A.; Taarning, E. *Green Chem.* **2012**, *14*, 702.
(19) Beletskiy, E. V.; Shen, Z.; Riofski, M. V.; Hou, X.; Gallagher, J. R.; Miller, J. T.; Wu, Y.; Kung, H. H.; Kung, M. C. *Chem. Commun.* **2014**, *50*, 15699.
(20) Wang, X.; Xu, H.; Fu, X.; Liu, P.; Lefebvre, F.; Basset, J.-M. *J. Mol. Catal. A: Chem.* **2005**, *238*, 185.
(21) Li, L.; Liu, J.; Su, Y.; Li, G.; Chen, X.; Qiu, X.; Yan, T. *Nanotechnology* **2009**, *20*, 155706.
(22) Yang, H.; Lu, Q.; Gao, F.; Shi, Q.; Yan, Y.; Zhang, F.; Xie, S.; Tu, B.; Zhao, D. *Adv. Funct. Mater.* **2005**, *15*, 1377.
(23) Parry, E. P. *J. Catal.* **1963**, *2*, 371.
(24) Mal, N. K.; Ramaswamy, A. V. *J. Mol. Catal. A: Chem.* **1996**, *105*, 149.
(25) de Graauw, C. F.; Peters, J. A.; van Bekkum, H.; Huskens, J. *Synthesis* **1994**, *1994*, 1007.
(26) Anwander, R.; Palm, C. *Stud. Surf. Sci. Catal.* **1998**, *117*, 413.
(27) Zhu, Y.; Chuah, G.; Jaenicke, S. *J. Catal.* **2004**, *227*, 1.
(28) Sushkevich, V. L.; Ivanova, I. I.; Tolborg, S.; Taarning, E. *J. Catal.* **2014**, *316*, 121.
(29) Luo, H. Y.; Consoli, D. F.; Gunther, W. R.; Román-Leshkov, Y. *J. Catal.* **2014**, *320*, 198.
(30) Lewis, J. D.; Van de Vyver, S.; Crisci, A. J.; Gunther, W. R.; Michaelis, V. K.; Griffin, R. G.; Román-Leshkov, Y. *ChemSusChem* **2014**, *7*, 2255.
(31) Tang, B.; Dai, W.; Wu, G.; Guan, N.; Li, L.; Hunger, M. *ACS Catal.* **2014**, *4*, 2801.

DOI: 10.1021/jacs.5b13436
J. Am. Chem. Soc. 2016, 138, 4294−4297